AIAA 80-0132R

Turbulence Models for High-Speed, Rough-Wall Boundary Layers

T. C. Lin*
TRW Systems Group, San Bernardino, Calif.
and
R. J. Bywater†
The Aerospace Corporation, El Segundo, Calif.

Three distinct approaches have been investigated for the calculation of heat, momentum, and mass transfer in rough-wall turbulent boundary layers. Emphasis is placed on the high-speed flow regime. Of particular interest is the turbulent kinetic energy model, which has been modified to incorporate a two-phase flow concept such that the formulation allows explicit consideration of the effects of roughness shape, pattern, and density. The assessment consists of comparisons between numerical results and experimental data. These preliminary results suggest the following: 1) a local roughness-induced heating reduction is possible in high-speed flow; 2) the specification of nominal roughness height alone is not sufficient to define the rough-wall geometry characteristics; and 3) a strong Mach number effect on rough-wall heat transfer and shear stress distributions may exist. More accurate and complete data are needed in the high-speed regime to verify advanced numerical models of the type considered herein, which are required to adequately predict high-speed rough-wall boundary-layer behavior.

Nomenclature

a,b = roughness elements spacing (see Fig. 1)
A = Van Driest damping constant
B,C = constants defined in Eq. (1)
C_f = drag coefficient
C_{f_0} = smooth-wall drag coefficient
d = roughness element local diameter
E,e = turbulent kinetic energy
h = heat-transfer coefficient
k = roughness height
k^+ = ku_τ/ν
K = thermal conductivity
K_t = eddy conductivity
$\mathfrak{L}$ = spacing between two adjacent roughness elements
ℓ = mixing length
ℓ^+ = $\ell u_\tau/\nu$
M = Mach number
Nu = Nusselt number
p = pressure
r = radial distance in cylindrical coordinate
Re_d = $(\rho u d/\mu)_{\text{ref}}$
Re_θ = $\rho_e u_e \theta/\mu_e$
St = Stanton number
T = temperature
T^* = recovery temperature
T_w = wall temperature
u,v = velocity components in the boundary-layer coordinate
u_τ = $(\tau/\rho)^{1/2}$
u^+ = u/u_τ
Δu = logarithmic velocity shift caused by roughness
V_w = mass injection velocity at the surface
x,y = boundary-layer surface coordinates
y^+ = yu_τ/ν
α = roughness elements occupied area/total area
γ = specific heat ratio
δ = boundary-layer thickness
Λ = $\int_0^k h(T^*-T_w)\,d/\mathfrak{L}^2(dy)$
μ = viscosity
μ_t = eddy viscosity
ν = μ/ρ
ρ = density
τ = shear stress
Ω = specific turbulent dissipation rate

Introduction

THE impact of wall roughness on the determination of boundary-layer properties has long been recognized. Although this specific topic has been the subject of extensive research, emphasis has been placed on the low-speed flow.

In Nikuradse's pioneering work[1] on turbulent incompressible flows through rough pipes, he introduced the concepts of the 1) hydraulically smooth (i.e., $k^+ \leq 5$), 2) transitionally rough ($5 < k^+ < 60$), and 3) fully rough ($k^+ > 60$) surfaces. Nikuradse's experimental measurements were devoted exclusively to commercial sand grain roughness. Therefore, the applicability of his results to other types of wall roughness is uncertain. Schlichting[1] introduced the idea of "equivalent sand grain roughness" such that Nikuradse's data on rough-wall skin friction still can be used.

The important experimental observation concerning the velocity profile is that the roughness effect is confined to the inner region of the boundary layer. The velocity defect law is still universally valid, even in the presence of surface roughness. The influences of roughness on the law of the wall are manifested by a shift in the logarithmic profile, i.e.,

$$u^+ = 2.5\log y^+ + C - \Delta u$$

or

$$u^+ = 2.5\log(y/k) + B(k^+) \tag{1}$$

where B = roughness functions and Δu = logarithmic velocity shift caused by roughness. For a fully rough wall, Eq. (1) assumes the form

$$u^+ = 2.5\log(y/k) + 8.5 \tag{2}$$

Usually, B and Δu are deduced from experimental measurements. Very little has been done to develop a physical

Presented as Paper 80-0132 at the AIAA 18th Aerospace Sciences Meeting, Pasadena, Calif., Jan. 14-16, 1980; submitted June 23, 1980; revision received Aug. 17, 1981.

*Staff Scientist. Member AIAA.
†Member of Technical Staff, Fluid Mechanics Department. Member AIAA.

model from which B can be derived. At the present time, it is fair to state that our total knowledge of the effect of sand grain roughness is contained in Eqs. (1) and (2). One subtle difficulty in using Eq. (1) is the uncertainty of specifying the origin of y such that a linear logarithmic relation can be established. However, it is generally true that $y=0$ is located between the top and the bottom of the roughness elements.

Lieppman and Goddard[2] were the first to notice that the skin friction of a fully rough wall can be evaluated from the form drag of individual protuberances. This observation is significant for many prediction schemes, including those of the present formulation.

When experimental results are presented to demonstrate the effects of roughness on heat transfer in low-speed flow, they are often reported in terms of a sublayer Stanton number[3] which, in a way, is analogous to the role played by the form drag for momentum transfer on rough walls.

The influence of compressibility on the roughness effects has been investigated by Goddard,[4] who reached the following conclusions: 1) for a fully rough and adiabatic wall, the compressibility effects are accountable through a reduction in the flow density at the wall with increasing Mach number; 2) the skin friction enhancement C_f/C_{f_0} is the same function of roughness Reynolds number k^+ as in an incompressible flow; and 3) the shift in the logarithmic velocity profile Δu is a function of k^+ and is again identical to the incompressible case. The implication of Goddard's results is that the effect of roughness for compressible flow can be formulated in a fashion similar to that of the incompressible case if the pertinent parameters are evaluated based on local flow properties at the wall.

Holden[5] has obtained rough-wall heat-transfer data in hypersonic flow ($M_\infty = 11.3$). His measurements reveal that the heat transfer on a slender cone at zero yaw is smaller on a 10 mil rough wall than on a smooth wall. These are unexpected results. Recently, another set of data taken at NSWC Tunnel 9[6] ($M_\infty = 10$) indicated that the heat transfer is always higher on rough walls. Obviously, these two sets of data lead to a completely different conclusion and cannot be explained based upon the previous knowledge of rough-wall boundary layers just discussed.

Most of the existing analytical work[7-12] is concentrated on the empirical correlation of heating augmentation with emphasis on the low-speed flow regime. Other more elaborate mathematical models are found in Refs. 13-19. Usually, these models were incorporated into a set of partial differential equations comprising a boundary-layer description for which finite-difference solutions were obtained. This made it possible to monitor model effects on boundary-layer structure via detailed boundary-layer profiles while making comparisons with skin friction or heating data. A certain degree of success has been achieved with these predictive techniques. However, one weakness in all these approaches is the neglect of the roughness patterns and density in their formulation.

The implication of the above survey is clear. A comprehensive and systematic study is needed of the effects of wall roughness on heat transfer for compressible turbulent flows.

This paper documents the results and experience obtained by using three different analytic models developed for the rough-wall turbulent boundary layer. The following formulations are considered: 1) the algebraic eddy viscosity model,[14] 2) the modified turbulent kinetic energy (TKE) equation, and 3) the Saffman-Wilcox model.[16] Among these three methods, the modified TKE model,[20] which is derived from the concept of two-phase flow, takes into account the roughness pattern and density distribution. These methods are assessed by comparing computed results with experimental data for high-speed flow. One of our goals is to resolve the anomalies introduced by the data of Holden and Hill. Furthermore, sample results for the roughness effects upon the surface pressure on a wedge are presented.

Formulation

In this paper, attention is restricted to roughness heights which are small compared to the boundary-layer thickness. As a consequence of this limitation, the boundary-layer assumptions remain valid, and calculation methods can be based on the boundary-layer equations. In terms of the mass-averaged mean quantities, the coupled set of equations describing compressible boundary-layer flow over axisymmetric bodies are as follows

$$(\rho u r)_x + (\rho v r)_y = 0$$

$$\rho u u_x + \rho v u_y = -p_x + \frac{1}{r}\frac{\partial}{\partial y}[(\mu+\mu_t) r u_y]$$

$$\rho C_v [u T_x + v T_y] + p\left[u_x + \frac{1}{r}(vr)_y\right] = \mu u_y^2 + \frac{1}{r}\frac{\partial}{\partial y}[(K+K_t) r T_y] \tag{3}$$

The corresponding boundary and initial conditions are

$$y=0, \quad u=v=0, \quad T=T_w \text{ or } T_y=0$$

$$y\to\infty, \quad u\to u_e, \quad T\to T_e$$

and $x=x_0$, $u=u(y)$, $T=T(y)$.

Three different methods shall be used to evaluate the eddy viscosity and eddy conductivity (i.e., μ_t and K_t).

Algebraic Model

The Reynolds stress is assumed to be proportional to the mean shear with the eddy viscosity as the proportionality factor, i.e.,

$$-\rho\overline{u'v'} = \rho\epsilon u_y \tag{4}$$

where $\epsilon = \ell^2 u_y$ and ℓ = mixing length. Over a smooth wall, the inner region of the boundary layer ℓ can be specified as

$$\ell = 0.4y[1-\exp(-y^+/A)] \tag{5}$$

where A = Van Driest damping constant, $y^+ = yu_\tau/\nu$, and $u_\tau = \sqrt{\tau/\rho}$. While in the outer region of the boundary layer, ℓ is assumed to be equal to 0.09δ. On a transitionally rough surface (i.e., $k^+ = ku_\tau/\nu_w < 60$), Healzer et al.[14] have proposed that the mixing length ℓ remains the same in Eq. (5), except A is modified by

$$A = 26(4.007 - \ell n k^+)/f, \quad k^+ > 2$$

where f is a surface material-dependent constant. For a fully rough wall, i.e., $k^+ > 60$, ℓ is further modified as

$$\ell^+ = \ell u_\tau/\nu_w = [(0.4y^+)^2 + [(k^+ - 46)/39]^2 - 0.05325]^{1/2}$$

In the Healzer et al. model, the effects of mass injection and pressure gradient are implicitly influenced by the evaluation of k^+.

Recently, Dahm[13] suggested a unified mixing length model for both smooth and rough walls with mass injection. His relation is derived from a large set of accurate data and assumes the following form

$$d\ell^+/dy^+ = [0.4y^+ - (\ell^+ - \ell_w^+] \times [1 + (V_w/u_\tau)(u/u_\tau)]^{1/2}/11.83$$

where ℓ_w is a constant that depends on k^+ only.

The eddy conductivity is calculated from the definition of turbulent Prandtl number, i.e.,

$$Pr_t = \mu_t C_p / K_t$$

Both $Pr_t = \text{const}$ and $Pr_t = Pr_t(y)$ are examined in the present formulation. In particular, Dahm's correlation for rough-wall turbulent Prandtl number is employed in the numerical computations.

Both the Healzer et al. formulation[14] and Dahm's model[13] assume the eddy viscosity is nonzero at the fully rough wall. Also, the location at which $y=0$ is somewhat uncertain. Dahm suggested setting $u=0$ at a distance of two-thirds the roughness height above the base of the roughness element. Finally, it should be pointed out that this simple algebraic model does not explicitly take into account the roughness shape, density, and pattern.

Saffman-Wilcox Model

In the Saffman and Wilcox[16] formulation, the eddy viscosity is evaluated from

$$\mu_t = E/\Omega$$

where E = turbulent kinetic energy and Ω = specific turbulent dissipation rate. Here, E and Ω are determined by the following differential equations, i.e.,

$$\rho u \frac{\partial E}{\partial x} + \rho v \frac{\partial E}{\partial y} = [C_1 \mid u_y \mid - C_2 \rho \Omega] \rho E + \xi E (u \rho_x + v \rho_y) + \frac{1}{r} \frac{\partial}{\partial y} \left[r \left(\mu + C_e \frac{E}{\Omega} \right) E_y \right] \tag{6}$$

and

$$\rho u (\Omega^2)_x + \rho v (\Omega^2)_y = [C_4 \mid u_y \mid - C_5 \rho \Omega] \rho \Omega^2 + \frac{1}{r} \frac{\partial}{\partial y} \left[r \left(\mu + C_3 \frac{E}{\Omega} \right) (\Omega^2)_y \right]$$

where $C_1 = 0.3$, $C_2 = 0.09$, $\xi = 2.5$, $C_3 = 0.5$, $C_4 = 0.333$, and $C_5 = 0.15$. Roughness effects arise through the specification of the boundary conditions, i.e.,

$$y=0, \quad E=0 \qquad \Omega = u_\tau^2 S_R (C_6 \mu)^{-1}$$

$$C_6 = 0.3 \qquad S_R = (36/k^+)^2 + (8/k^+)^{1/2} \tag{7}$$

The physical interpretation of these surface boundary conditions is that the presence of wall roughness results in a vortical layer near the surface. However, as $y \to 0$, μ_t approaches zero as well. Note that in this model there is no need to specify the length scale ℓ. Herein, the specification of ℓ is replaced by the calculation of Ω and the specification of several constants in its governing equations.

Modified TKE Equation Model—A Two-Phase Flow Model

This method employs the concept of two-phase flows to evaluate the flow properties over the rough wall. In terms of the mass-averaged mean quantities, the basic equations describing the compressible boundary-layer flow are

$$[\rho u r (1-\alpha)]_x + [\rho v r (1-\alpha)]_y = 0 \tag{8}$$

$$(1-\alpha)\rho u u_x + (1-\alpha)\rho v u_y + (1-\alpha) p_x = \frac{1}{r} \frac{\partial}{\partial y} (1-\alpha)(\mu + \mu_t) r u_y - \underline{\tfrac{1}{2} \rho u^2 C_D \frac{d}{\mathcal{L}^2}} \tag{9}$$

$$p_y = 0$$

and

$$(1-\alpha)\rho u C_v T_x + (1-\alpha)\rho v C_v T_y + (1-\alpha) p [u_x + (vr)_y r^{-1}] = \frac{1}{r} \frac{\partial}{\partial y} (k + k_t)(1-\alpha) r T_y + (1-\alpha)\mu u_y^2 + \underline{h (T^* - T_w) \frac{d}{\mathcal{L}^2}} + \underline{\tfrac{1}{2} \rho C_D u^3 \frac{d}{\mathcal{L}^2}} \tag{10}$$

where

α = solid-phase area ratio = roughness area/total area
$\mathcal{L}$ = average center-to-center spacing of roughness elements
d = roughness element cross-sectional diameter
h = heat-transfer coefficient
T^* = adiabatic wall temperature
C_D = form drag coefficient

The eddy viscosity and eddy conductivity are expressed in terms of the TKE, e, and the turbulent Prandtl number Pr_t, i.e.,

$$-\rho \overline{u'v'} = \mu_t u_y = \rho C_\mu \ell e^{1/2} u_y$$

$$Pr_t = \mu_t C_p / K_t, \qquad C_\mu = 0.2383 \tag{11}$$

where e is calculated from the following equation:

$$\begin{aligned}(1-\alpha)\rho u e_x + (1-\alpha)\rho v e_y &= (1-\alpha)\rho e^{1/2} \ell C_\mu u_y^2 \\ &+ (1-\alpha)\,[3.93\mu (e/\ell^2) + \rho C_{10} (e^{3/2}/\ell)] \\ &+ \frac{1}{r} \frac{\partial}{\partial y} (\mu + \mu_t)(1-\alpha) r e_y - (8/9) e^{1/2} p_x (1-\alpha) \\ &+ \rho e (u_x + v_y + v/r)(C_{11} M^2/\gamma - 2/3)(1-\alpha) \\ &+ q_u \rho u^3 (d/\mathcal{L}^2)\end{aligned} \tag{12}$$

where $C_{10} = 0.3777$, $C_{11} = 8/11$, M is the local Mach number, γ the specific heat ratio, ℓ the characteristic turbulence length scale, $q_u = 0.04$, and

$$\ell_{\text{inner}} = \ell_w + 0.41y + 4.85\mu_w (e^{-y^+/11.83} - 1)/\rho u_\tau$$

$$\ell_{\text{outer}} = 0.2069\delta$$

where ℓ_{inner} and ℓ_{outer} are used for ℓ in their respective regions of validity. The term $q_u \rho u^3 (d/\mathcal{L}^2)$ represents the TKE generation which occurs due to the wakes of the roughness elements. A dissipation term could also be included; however, Finson and Wu[15] found that it had little effect upon the turbulent flow properties.

The boundary conditions for e are estimated from the one-dimensional Couette flow approximation which yields

$$\sqrt{e_w} = (\mu_t/\rho\ell)_w C_\mu^{-1}$$

$$(\mu_t)_w = \mu_w/2\,[(1 + 4\ell_w^{+2})^{1/2} - 1]$$

$$\ell_w^+ = [1.28 + 0.014k^+]\,[1 - \exp(-k^+/37)] \times [1 - \exp(-k^+/2)]^{1/4}$$

Here, ℓ_w is estimated from Dahm's correlation which was deduced from the data of Nikuradse and Healzer et al. Equations (9) and (10) are essentially the basic system for two-phase flows. Herein, the solid phase is always stationary (i.e., $u_s = 0$, $T_s = T_w$). The extra terms, underlined in Eqs. (9) and (10), represent the form drag and heat sink due to the existence of the roughness elements. In general, the local drag coefficient C_D and heat-transfer coefficient h depend on the local flow Mach number, Reynolds number, wall temperature, roughness dimension, and roughness density. In this formulation, the effects of roughness pattern and density are modeled through α, d, $\mathcal{L}$, C_D, and h.

Lieppman and Goddard were the first to recognize that the skin friction of a fully rough wall can be estimated from the

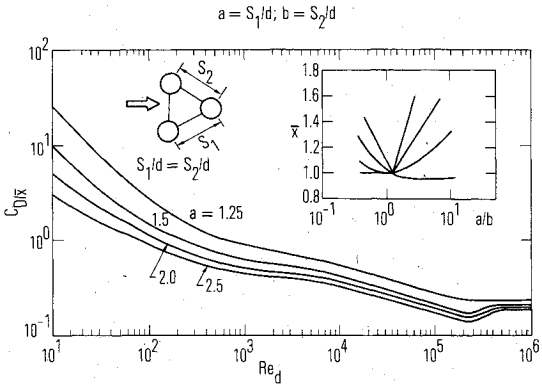

Fig. 1 Drag coefficient vs Re_d for staggered banks of tubes.

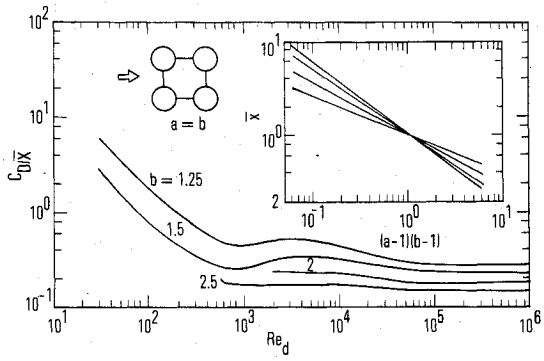

Fig. 2 Drag coefficient vs Re_d for in-line banks of tubes.

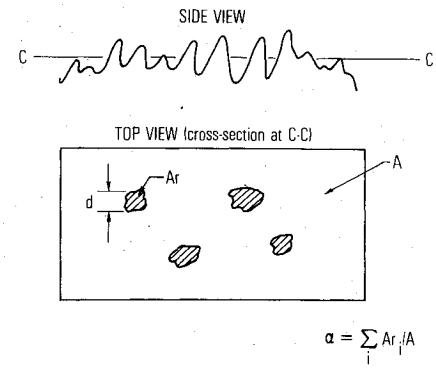

Fig. 3a Schematics of two-phase flow model for rough-wall boundary layers.

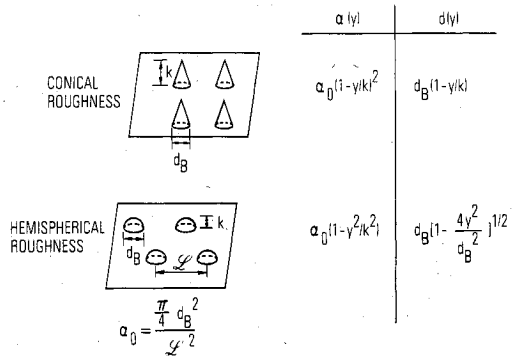

Fig. 3b Simple coefficients for various roughness characteristics.

drag of individual roughness elements. Finson and Wu, as well as Adams and Hodge, have incorporated this idea into their formulation. However, the convective heat-transfer term, i.e., $h(T^*-T_w)$, was not included. Also, their model is asymptotic to ours only in the limit of the void ratio $\alpha \to 0$. An analytical model similar to Eqs. (9) and (10) has been used by Chen et al.[21] to study the phenomena of transition from laminar to turbulent flow. But they too neglected the convective heat transfer between the roughness element and the gas.

The two-phase flow model employed in the turbulent kinetic energy equation model also can be incorporated into the other two formulations (i.e., Saffman's model and the algebraic eddy viscosity model). However, it is not clear how the existing empirical correlations [i.e., Eq. (7)], developed for the rough-wall Saffman and Wilcox model, would be modified in the two-phase flow approach. A deeper consideration appears necessary before those models are combined with the two-phase flow concept. On the other hand, the modified TKE formulation is considered to possess the potential for exploring problems with turbulent nonequilibrium effects. Also, the Mach number effects are explicitly included in the equation of the TKE model. Based on this reasoning, the TKE model in the two-phase flow approach was adopted for this study.

Definitions of C_f, St, h and C_D

Before the numerical results are discussed, definitions of rough-wall shear stress and Stanton number shall be defined. For the algebraic eddy viscosity and Saffman-Wilcox models, C_f and St are calculated from the following relation

$$C_f = \left[(\mu+\mu_t) \frac{\partial u}{\partial y} \right]_w \Big/ (\tfrac{1}{2}\rho_e u_e^2)$$

$$St = [(K+K_t)T_y]_w / \rho u (C_p T^* - C_p T_w)$$

In the Saffman-Wilcox formulation, $\mu_t = K_t = 0$ at $y=0$. In the modified TKE model, these definitions become

$$C_f = \left\{ (1-\alpha)(\mu+\mu_t)u_y + \int_0^k \tfrac{1}{2}\rho u^2 C_D \frac{d}{\mathscr{L}^2}\,dy \right\} \Big/ \tfrac{1}{2}\rho_e u_e^2$$

$$St = \left\{ (1-\alpha)(K+K_t)T_y + \int_0^k h(T^*-T_w)\frac{d}{\mathscr{L}^2}\,dy \right\} \Big/ [\rho u (C_p T^* - C_p T_w)]$$

The form drag coefficients C_D, used in Eq. (9), are depicted in Figs. 1 and 2 which are obtained from Zukauskas' experimental results[22] for flows through banks of tubes. The corresponding heat-transfer coefficient h is evaluated from the Nusselt number, i.e.,

$$Nu = hd/K$$

and the values of Nu are determined from the measurements of Ref. 22 which are summarized below

1) $10 < Re_d = ud(\rho/\mu)_{\text{ref}} < 100$

$$Nu = 0.8 Re_d^{0.4} Pr^{0.36}$$

2) $10^2 < Re < 10^3$

$$a/b < 2, \quad Nu = 0.35 (a/b)^{0.2} Re_d^{0.6} Pr^{0.35}$$

$$a/b > 2, \quad Nu = 0.4 Re_d^{0.6} Pr^{0.36}$$

Here, a/b represents the effects of roughness spacing (see Figs. 1 and 2).

3) $10^3 < Re < 2 \times 10^6$

$$Nu = 0.27 Re_d^{0.63} Pr^{0.36}$$

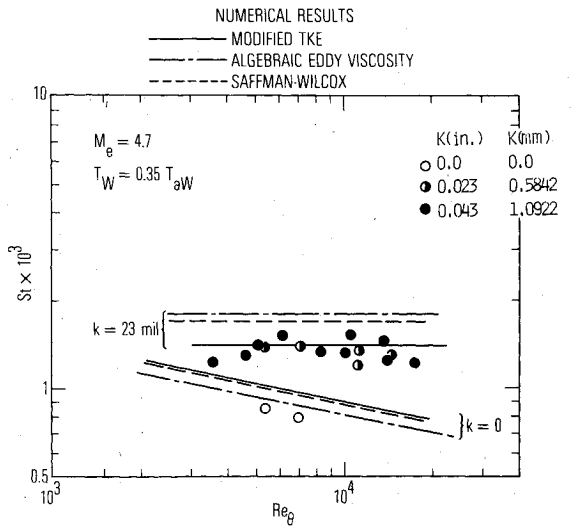

Fig. 4 Comparison of three methods in predicting surface heat transfer (Keel's data).

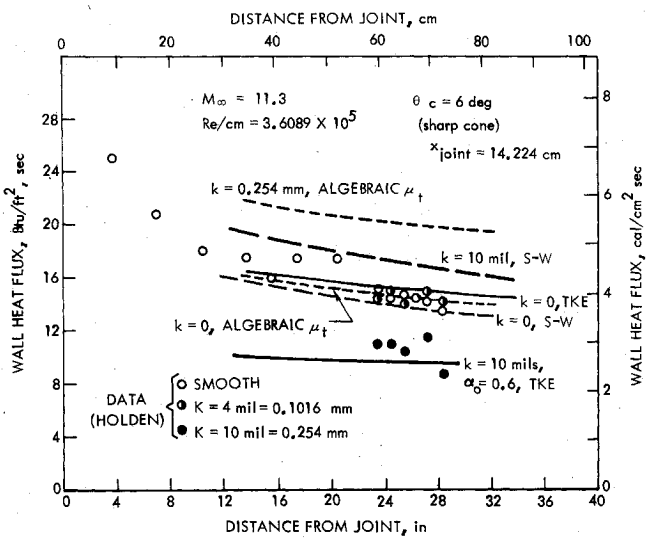

Fig. 5 Comparison of three methods in predicting surface heat transfer (Holden's data).

The gas properties in the above expressions are evaluated at the Eckert reference temperature.

The definition of roughness void ratio $1-\alpha$ is illustrated in Fig. 3. For simplicity, two types of roughness elements are considered: the hemispherical and conical shapes (see Fig. 3).

Results and Discussion

Numerical Solution of the Governing Equations

The governing compressible, time-averaged boundary-layer equations are discretized into linearized finite-difference forms. These are solved by an iterative, implicit marching integration scheme based on tridiagonal matrices. Full details of the numerical approach may be found in Ref. 23.

Figure 4 depicts the Stanton number on a 5 deg sharp cone with a freestream Mach number of 5 as predicted by the three methods. Both smooth- and rough-wall results are presented and compared with Keel's experimental results.[24] The three methods predict the smooth-wall heat transfer within 15% of the data, with the algebraic model giving the best estimate of the heating. When the numerical models are extended to the rough-wall case ($k = 23$ mil), the predictions are within 20% of the data. It is interesting to observe that Keel's measurements indicate no significant difference in heat transfer and shear stress between $k = 23$ and 43 mil (where 1 mil = 0.0000254 m).

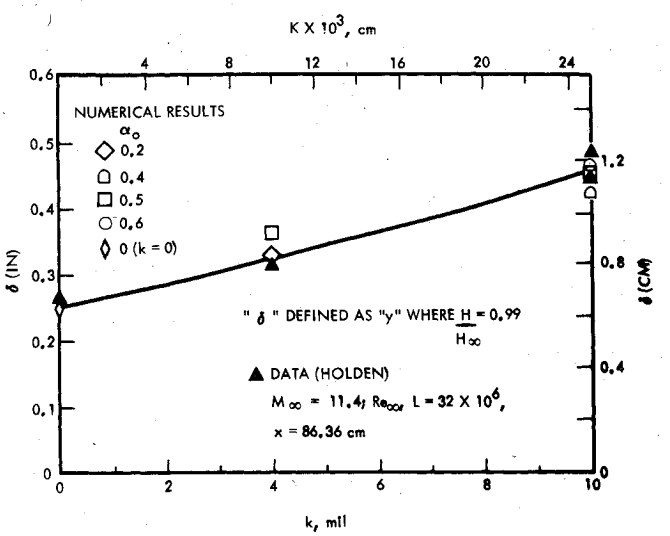

Fig. 6 Prediction of boundary-layer thickness by modified TKE model.

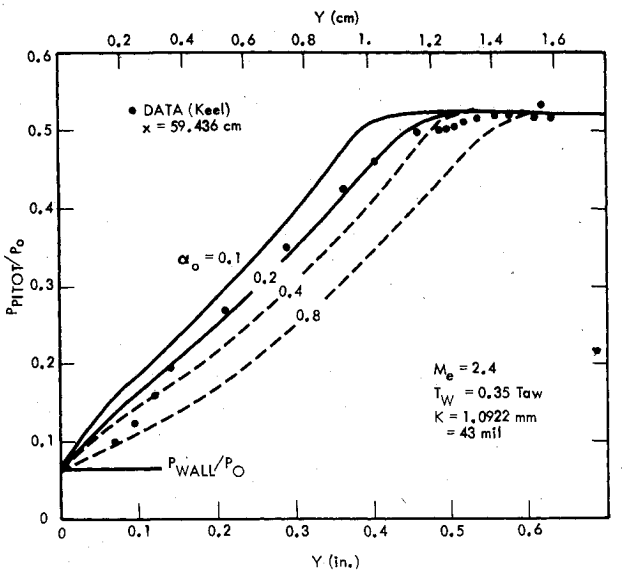

Fig. 7 Computed pitot pressure profiles by modified TKE model.

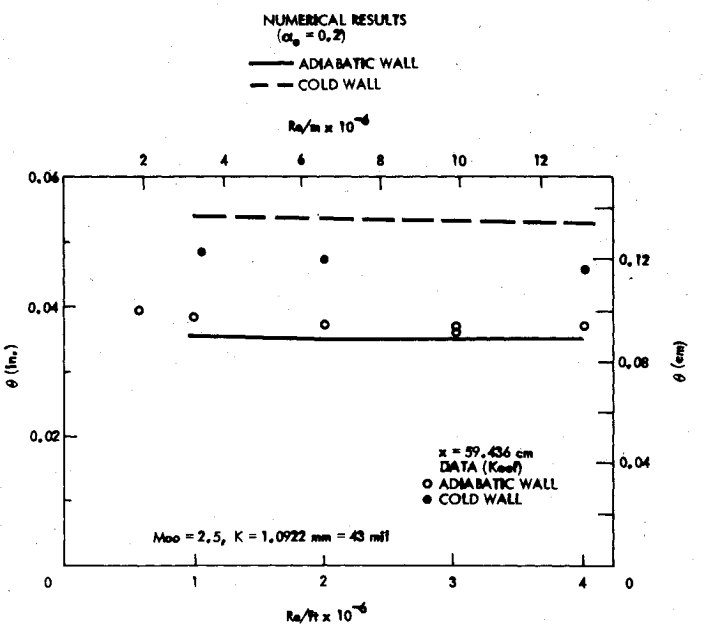

Fig. 8 Momentum thickness distribution for Keel's case.

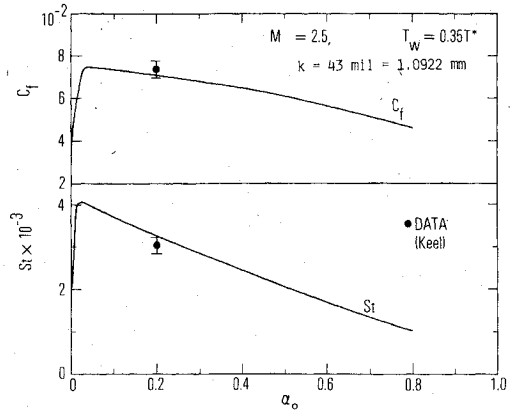

Fig. 9 Predictions of surface heat transfer and shear stress by modified TKE model.

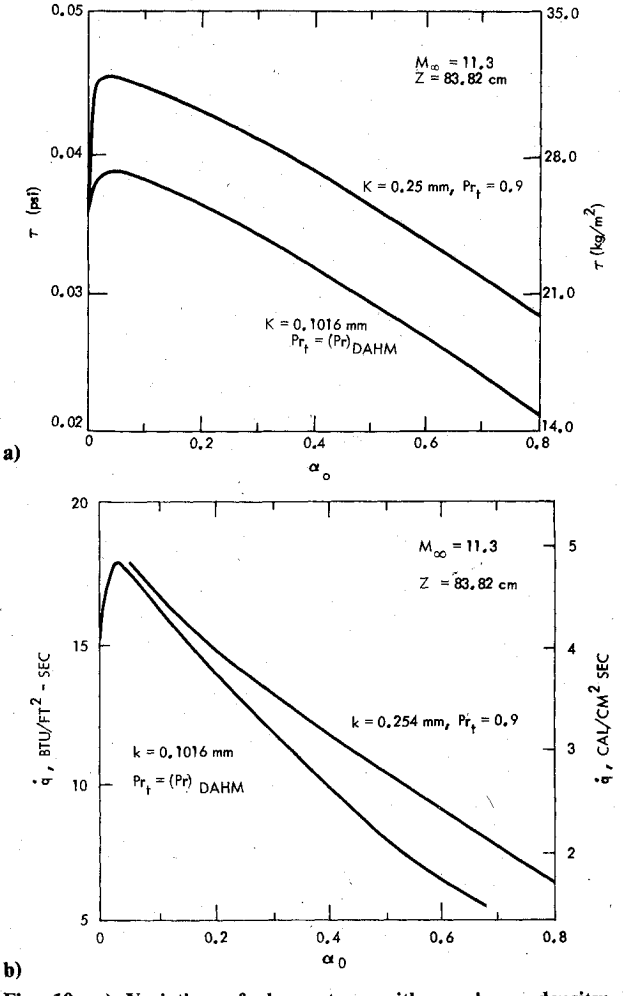

Fig. 10 a) Variation of shear stress with roughness density; b) variation of surface heat transfer with roughness density.

A comparison of numerical results with Holden's experimental measurements is illustrated in Fig. 5. One of the models in Ref. 5 is a 6 deg sharp cone, and the freestream conditions correspond to $M_\infty = 11.3$ and $Re/\text{cm} = 3.61 \times 10^5$. The algebraic and Saffman-Wilcox models predict a heating augmentation on the rough wall. Only the modified TKE model predicts a slight decrease (20%) in heat transfer when the roughness elements are 10 mil high. This is an interesting result since Holden's data also suggest the trend, i.e., surface heating is lower on the 10 mil rough wall than on the smooth surface. Based on this observation, further studies were conducted with the modified TKE model and are reported below.

Table 1 Roughness characterization[25]

Parameters	Grit-blasted surface, mm	Bonded-grit surface, mm
k_{min}	2.286×10^{-3}	2.286×10^{-3}
k_{max}	0.1486	0.15088
k_{mean}	0.41326	0.05085
k_{rms}	0.05649	0.063
σ_k	0.03881	0.03736
$\mathcal{L}_{min}$	0.03114	0.01676
$\mathcal{L}_{max}$	0.4745	0.2659
$\mathcal{L}_{mean}$	0.19479	0.0984
$\mathcal{L}_{rms}$	0.2292	0.1095
$\sigma_{\mathcal{L}}$	0.1227	0.04841

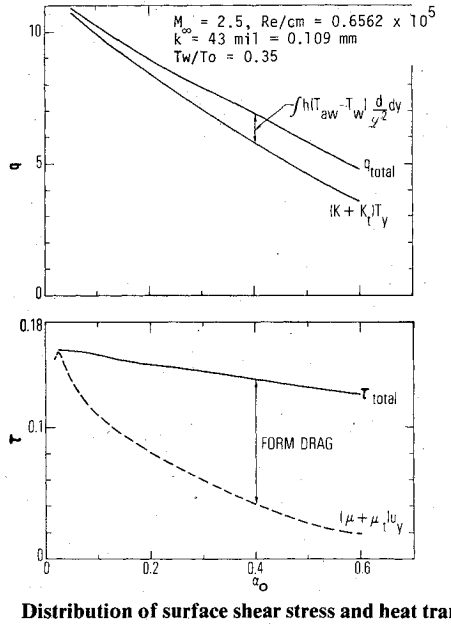

Fig. 11 Distribution of surface shear stress and heat transfer.

Determination of α

In the modified TKE model, it is necessary to specify the roughness density which is defined as α = roughness occupied area/total area. The value of α can be determined from the profilometer measurements (e.g., Ref. 25). When this information is not available, α can be determined by comparing the numerical results with experimentally measured boundary-layer thicknesses or pitot profiles. For instance, Holden[5] has measured the boundary-layer thickness on the cone surface (see Fig. 6). A series of numerical computations was made with α as a parameter. Figure 6 depicts the δ distribution for several values of α. It is found that $\alpha = 0.2$ and 0.6 will fit Holden's 4 and 10 mil data, respectively. These α values were used in estimating the heat transfer and shear stress for Holden's tests.

In the case of Keel's data, no measurement was made of boundary-layer thickness. However, Keel has presented the pitot profiles ($k = 43$ mil) and the inferred momentum thickness distribution. Figure 7 illustrates the predicted pitot profiles for different values of α. The data in Ref. 24 is also shown. Here, the modified TKE model gives the best agreement with data for $\alpha = 0.2$. With $\alpha = 0.2$, the correspondingly predicted momentum thicknesses are shown in Fig. 8, and it compares reasonably well with Keel's inferred θ values. Unfortunately, Keel did not present any pitot profile data for the $k = 23$ mil case. As a result of this exercise, $\alpha = 0.2$ is assumed to correspond to $k = 23$ mil.

Experimental Information on the α Distribution

Although Holden's and Hill's data are similar in freestream conditions and model geometry, differing conclusions

regarding roughness effects (i.e., heating augmentation or reduction) can be deduced from their measurements. Certain subtle differences exist between these two sets of data. For instance, Holden applied the thin-film technique to measure the heat transfer, while Hill used thermocouples. Also, the methods of inserting the roughness elements on the model surfaces differed somewhat. In Ref. 25 an extensive investigation was conducted on the characteristics of grit-blasted and bonded-grit surfaces.

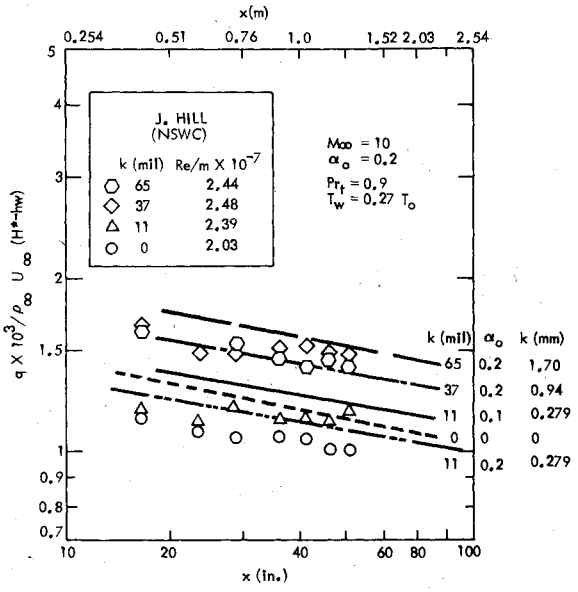

Fig. 12 Prediction of surface heat transfer by modified TKE model (Hill's data).

Foster, Read, and Murray[25] measured the roughness height, spacing, shape, and density. Statistical analyses were used to find the mean and standard deviations. Table 1 (obtained from Ref. 25) suggests an interesting result. Note that the roughness density can be significantly different as reported by the two methods, even for similar roughness heights. For example, the bonded-grit surface gives

$$\alpha = (\pi/4)d^2/\mathcal{L}^2 = 0.677$$

while the grit-blasted surface yields $\alpha = 0.191$. In this specific example, we find that the α for the bonded-grit surface is significantly larger than that for the grit-blasted surface, even though their k_{rms} are about the same.

Variation of C_f and St with α

Figures 9 and 10 depict the variation of surface heat transfer and drag with respect to α for the Holden and Keel cases, respectively. In the low Mach number case ($M_\infty = 2.5$), note that rough-wall shear stress is always larger than smooth-wall values, no matter what the magnitude of α is. The rough-wall Stanton number can be lower than the smooth-wall when $\alpha > 0.6$. For hypersonic flow the smooth-wall surface drag and heating can be larger than their rough-wall counterpart when α assumes certain values (see Fig. 10). This trend suggests a Mach number effect.

There are several contributors to the surface drag and heat transfer. This is demonstrated in Fig. 11 which indicates that the form drag term [i.e., $\int \frac{1}{2}\rho u^2 C_D(d/\mathcal{L}^2)dy$] is the im-

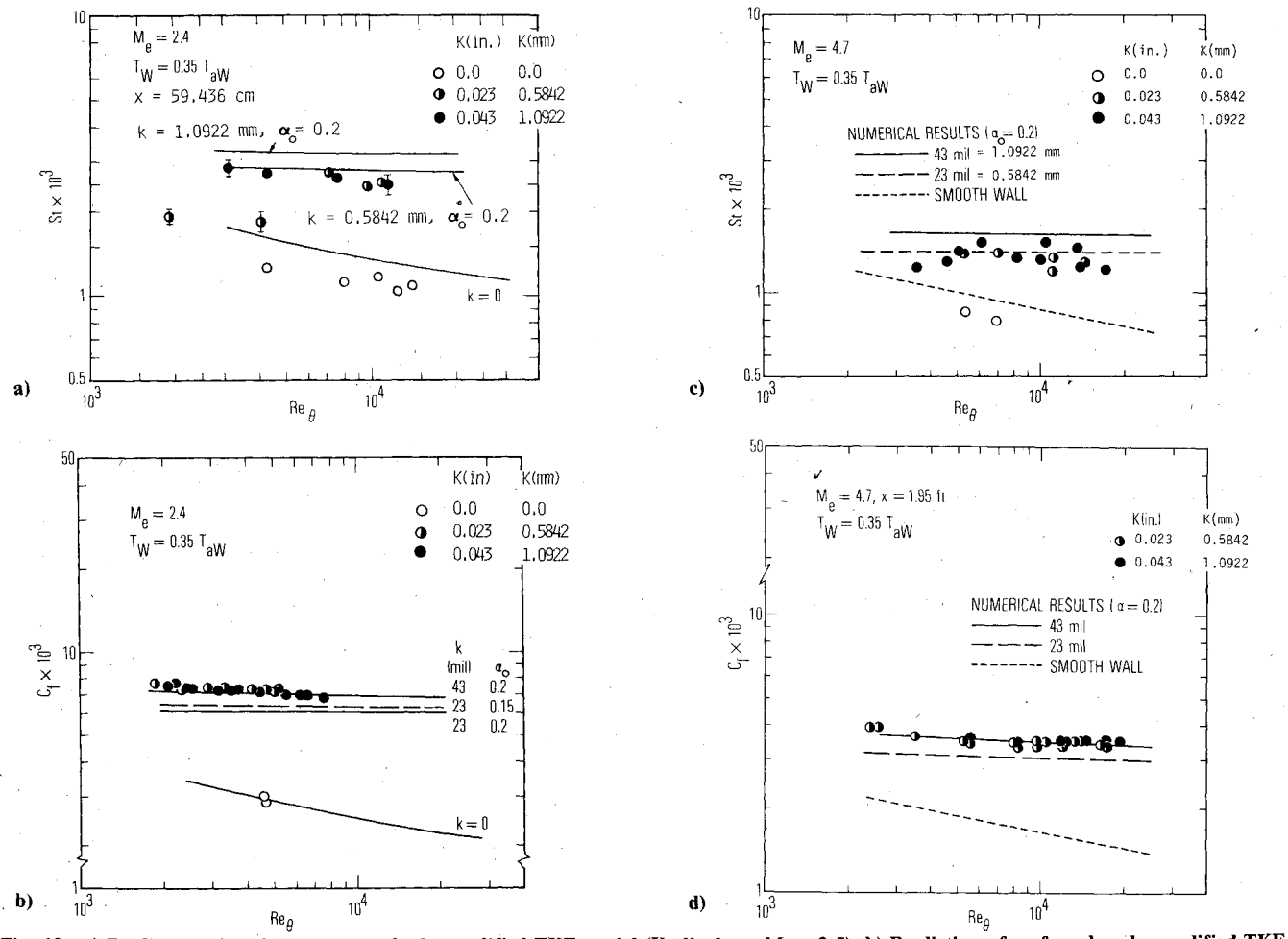

Fig. 13 a) Prediction of surface heat transfer by modified TKE model (Keel's data, $M_\infty = 2.5$). b) Prediction of surface drag by modified TKE model (Keel's data, $M_\infty = 2.5$). c) Prediction of surface heat transfer by modified TKE model (Keel's data, $M_\infty = 5$). d) Prediction of surface drag by modified TKE model (Keel's data, $M_\infty = 5$).

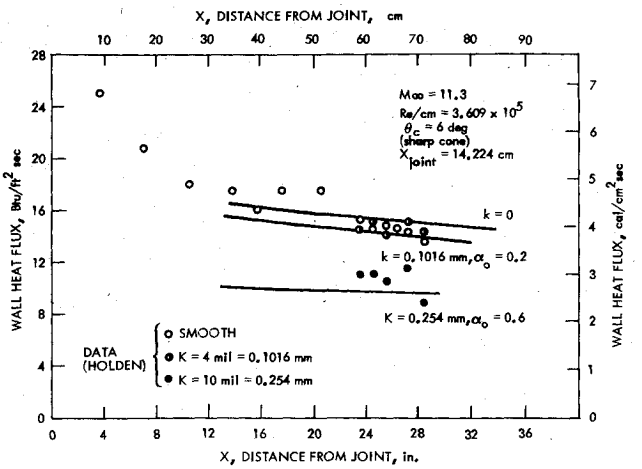

Fig. 14a Prediction of surface heat transfer by modified TKE model (Holden's data).

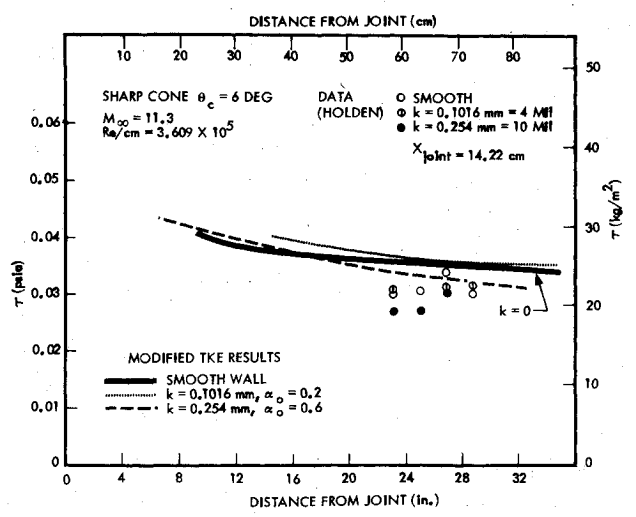

Fig. 14b Prediction of surface drag by modified TKE model (Holden's data).

portant contributor to the drag when $\alpha > 0.2$. This conclusion is consistent with Lieppman's experimental observations. On the other hand, the convective heat-transfer term for the roughness elements [i.e., $\Lambda = \int h(T^* - T_w)(d/\mathcal{L}^2)dy$] is not dominant as is the momentum sink term. However, it should not be ignored completely, because Λ still contributes to 20% of the total heat transfer at $\alpha = 0.5$.

Predictions for Hill's Data

The freestream conditions for Hill's data resemble Holden's test environments. His test model consists of a 7 deg cone more than 1.5 m (5 ft) long. Hill did not measure the pitot profiles or the boundary-layer thickness; therefore, under the present formulation, we could not determine the value of roughness density α. Since Hill's rough-wall cones presumably were made similar to Keel's model, it is reasonable to use the same value of $\alpha = 0.2$ in the prediction of Hill's data.

Figure 12 depicts the comparison between the NSWC Tunnel 9 results and the prediction of the modified TKE model. The predictions of heating augmentation agree reasonably well with experimental measurements at $k = 65$ and 37 mil. The modified TKE model overpredicts the smooth-wall heat transfer by 10%, and it also suggests that a heating reduction would occur for a 11 mil rough wall with $\alpha = 0.2$. Hill's data indicate a heating augmentation of $k = 11$ mil (see Fig. 13).

It should be noted that the roughness density α is unknown. For example, if $\alpha = 0.1$ is assumed in the case of $k = 10$ mil, a slight heating augmentation is predicted by the modified TKE model (see Fig. 12).

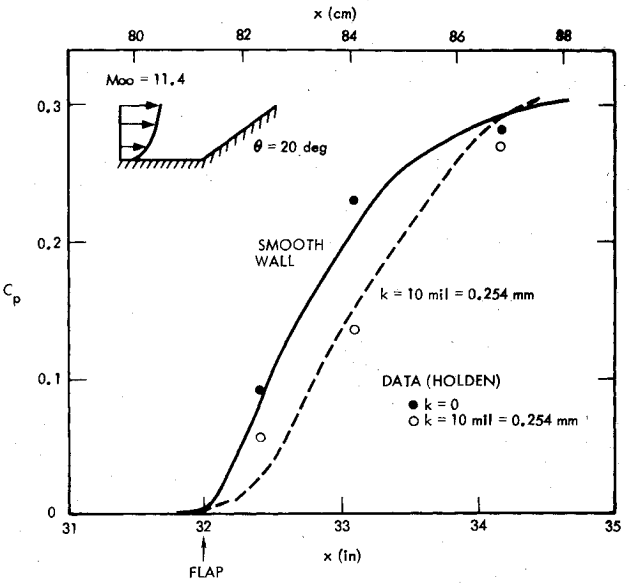

Fig. 15 Flap surface pressure distribution.

Predictions for Keel's Data

Keel's model consists of a 5 deg sharp cone upon whose surface is distributed uniform sand grain roughness. Tests were conducted at freestream Mach numbers of 2.5 and 5, and length Reynolds numbers of $1\text{-}25 \times 10^6$. Experimental data include the $\dot{q}$, τ, and pitot pressure profiles. The heat-transfer measurements were obtained with a slug calorimeter-type gage, and the skin friction data were made with internally mounted, floating element skin friction balances.

The modified TKE model's predictions on pitot pressure profiles and the momentum thickness distributions for the $k = 43$ mil case are presented in Figs. 7 and 8. The predicted St and C_f are depicted in Fig. 13 which includes the cases of $M_\infty = 5$ and 2.5. From these figures, note that the variations of rough-wall St (or C_f) with respect to Re_θ are weak. The numerical results agree reasonably well with Keel's data. It is interesting to observe there is no discernible difference in heat-transfer and shear stress data between the $k = 43$ and 23 mil cases. The analytical predictions suggest the St for $k = 43$ mil ($\alpha = 0.2$) would be 10% larger than the case for $k = 23$ mil ($\alpha = 0.2$). As mentioned earlier, the roughness density is not known for the $k = 23$ mil case (since there is no pitot pressure measurement). The agreement between the experimental data and the theoretical prediction is improved if $\alpha = 0.15$ is used for the $k = 23$ mil case (see Fig. 13b).

Predictions for Holden's Data

The test model is a 6 deg cone with uniformly distributed roughness. The freestream conditions are $M_\infty = 11.3$ and $Re/\text{cm} = 3.61 \times 10^5$. The heat-transfer measurements were obtained by the Calspan thin-film technique, and the drag measurements were made by floating strain gage balances.

Holden has measured the boundary-layer thickness distribution which is illustrated in Fig. 6. The modified TKE model predictions on δ are also shown in Fig. 6 as a comparison. The surface heat-transfer and drag measurements are depicted in Fig. 14. This set of data is unique and controversial, since it indicates that roughness would decrease both the heat transfer and skin friction relative to that on a smooth wall. The present theoretical model does predict the roughness-induced heating and drag reductions. The agreement between the experimental data and the numerical results on heat transfer is encouraging. Our theoretical results on wall shear stress overpredicts the data by 15-20%. Some of Holden's measurements are not in the fully rough regime (i.e.,

$k^+ < 70$). This implies the need for further investigation, since transitionally rough phenomena may have significant influence on the type of heat-transfer reduction being observed.

Roughness Effects on Flap Pressure

One technology issue for missiles using flap controls is the effect of boundary-layer characteristics on flap performance. Inviscid flow finite-difference calculations have been performed with the initial profiles ahead of the ramp consisting of a composite solution of the inviscid flow and the supersonic portion of the turbulent shear flow. Sample results are demonstrated in Fig. 15 for a flap of 20 deg. Note that the wall roughness significantly decreases the flap surface pressure initially. Holden's data are also shown in Fig. 15. The present numerical model predicts the flap wall pressure distribution reasonably well, demonstrating an important applications area in this type of modeling effort. With local surface pressure reductions approaching 35%, the present model could prove a valuable design tool.

Summary

Three distinct methods were used to study the rough-wall boundary-layer properties, with emphasis on the high-speed flow regime. Attention is focused on a turbulent kinetic energy model which has been modified to include the two-phase flow formulation. It allows explicit consideration of the effects of roughness shape, pattern, and density. The preliminary results suggest the following: 1) a local roughness heating reduction is possible in high-speed flow; 2) the specification of the nominal height of roughness alone is not sufficient to define the rough-wall characteristics; 3) the roughness element form drag is the major contributor to the rough-wall shear stress; 4) there may be a strong Mach number effect on rough-wall heat-transfer and shear stress distributions; and 5) surface roughness may significantly reduce the surface pressure on the initial portion of a high-speed flap.

Our numerical results also imply that more accurate and complete data are needed in the high-speed flow regime to test advanced numerical models of the type considered herein which are required for more reliable predictions. The experimental measurement should include surface pressure, heat transfer, wall shear stress, pitot pressure profiles, and total temperature distributions.

In summary, the present modeling effort has provided an explanation for anomalous heat-transfer phenomena. The present approach has demonstrated the capacity for discerning some rather subtle roughness pattern associated phenomena in the high-speed flow regime. In addition, it has been illustrated how the added flexibility and detail of the present approach can be used to define test regimes critical to the understanding of roughness effects.

Acknowledgment

This study was supported by the Air Force Ballistic Missile Office under Contract F04704-80-C-0021.

References

[1] Schlichting, H., *Boundary Layer Theory,* McGraw Hill Book Co., New York, 1961.

[2] Lieppman, H. W. and Goddard, F. E. Jr., "Note on the Mach Number Effect upon the Skin Friction of Rough Surfaces," *Journal of Aeronautical Sciences,* Vol. 24, March 1957, p. 784.

[3] Owen, P. R. and Thompson, W. R., "Heat Transfer Across Rough Surfaces," *Journal of Fluid Mechanics,* Vol. 25, March 1963, pp. 321-334.

[4] Goddard, F. E. Jr., "Effects of Uniformly Distributed Roughness on Turbulent Skin-Friction Drag at Supersonic Speeds," *Journal of Aerospace Sciences,* Vol. 26, Jan. 1959, pp. 1-15.

[5] Holden, M., "Studies of Aero-Thermodynamic Phenomena Influencing the Performance of Hypersonic Re-Entry Vehicles," SAMSO-TR-79, Calspan Corp., Buffalo, N. Y., April 1979.

[6] Hill, J., Personal communication, Naval Surface Weapons Center, July 1979.

[7] Fenter, F. W., "The Turbulent Boundary Layer on Uniformly Rough Surfaces at Supersonic Speeds," University of Texas, Austin, Tex., Rept. DRL-437, Jan. 1960.

[8] Nestler, D. E., "Compressible Turbulent Boundary Layer Heat Transfer to Rough Surface," AIAA Paper 70-742, June 1970.

[9] "Passive Nosetip Technology (PANT) Program," SAMSO-TR-74-86; also, C. A. Powars et al., "Surface Roughness Effects on Reentry Heating," Aerotherm TM-71-10, July 1971.

[10] Seidman, M. H., "Rough Wall Heat Transfer in a Compressible Turbulent Boundary Layer," AIAA Paper 78-163, Jan. 1978.

[11] Chen, K. K., "Compressible Turbulent Boundary Layer Heat Transfer to Rough Surfaces in Pressure Gradient," *AIAA Journal,* Vol. 10, May 1972, pp. 623-629.

[12] Dirling, R. B. Jr., "A Method for Computing Rough Wall Heat Transfer Rates on Reentry Nosetip," MDAC Paper WD1778 presented at AIAA 8th Thermophysics Conference AIAA Paper 73-763, Palm Springs, Calif., 1973.

[13] Dahm, T., Personal communication, Aerotherm/Acurex Corp., Aug. 1979.

[14] Healzer, J. M., Moffat, R. J., and Kays, W. M., "Turbulent Boundary Layer on a Rough Porous Plate: Experimental Heat Transfer with Uniform Blowing," Stanford University, Stanford, Calif., Rept. HMT-18, 1974.

[15] Finson, W. L. and Wu, P. K. S., "A Reynolds Stress Model for Boundary Layer Transition with Application to Rough Surfaces," PSI-TR-34, Aug. 1975; also, AIAA Paper 79-8, Jan. 1979.

[16] Wilcox, D. C. and Chambers, T. L., "Further Refinement of Turbulence-Model and Transition-Prediction Technique," DCW-TR-03-02, July 1975.

[17] Adams, J. and Hodge, B. K., "The Calculation of Compressible Transitional, Turbulent and Relaminarizational Boundary Layers over Smooth and Rough Surfaces using an Extended Mixing-Length Hypothesis," AEDC-TR-77-96, Feb. 1978.

[18] Cebeci, T. and Chang, K. C., "Calculation of Incompressible Roughwall Boundary-Layer Flows," *AIAA Journal,* Vol. 16, July 1977, pp. 730-735.

[19] Reeves, B. L., "Two-Layer Model or Rough Wall Turbulent Boundary Layer," AIAA Paper 75-191, Jan. 1975.

[20] Rubesin, M. W., "A One-Equation Model of Turbulence for Use with the Compressible Navier-Stokes Equations," NASA-TM-X-73, April 1976, p. 128.

[21] Chen, K., Zavasky, J., Serp, P., and Liu, T., "Nosetip Shape Regimes: Laminar Boundary Layer with Roughness," SAMSO-TR-75-269, Oct. 1975.

[22] Zakauskas, A., "Heat Transfer from Tubes in Crossflow," *Advances in Heat Transfer,* edited by J. P. Hartnett and T. F. Irvine, Academic Press, New York, 1972.

[23] Lin, T. C. and Rubin, S. G., "A Two-Layer Model for Coupled Three-Dimensional Viscous and Inviscid Flow Calculations," AIAA Paper 75-853, June 1975.

[24] Keel, A. G. Jr., "Influence of Surface Roughness on Compressible Turbulent Boundary Layer with Heat Transfer," AIAA Paper 77-178, Jan. 1977.

[25] Foster, T., Reed, D., and Murray, A., "Surface Roughness Heating Augmentation Tests in AEDC-Tunnel F," Acurex Rept. TR-78-183, June 1979.